Analysis on Micro-Mechanical State at Tip of Stress Corrosion Cracking in Nickel base Alloy

Xue He [1], Yongqiang Li [1], Yinghao Cui [1] & Zheng Chen [1]

[1] Department of School of Mechanical engineering, Xi'an University of Science & Technology, Xi'an 710054, China

Key words: Nickel base alloy; stress corrosion cracking; oxide film; groove-type crack; FEM.

Abstract. It is one of the main failure forms that stress corrosion cracking (SCC) of nickel base alloys and stainless steels in the nuclear pressure vessels and piping. Current researches show that SCC is a process of oxide film rupture and reform. To understand the micro-mechanical state at the SCC crack tip, the stress distribution in oxide film and base metal is analyzed before and after the oxide film rupture, and the effect of groove-type crack length on the stress field at SCC crack tip is also discussed in this paper. The investigated results provide a new insight into the mechanism of SCC growth of the nuclear structural materials in a high water environment.

1.Introduction

Nickel base alloys and stainless steels have been widely used as structural materials in nuclear power equipments due to their good corrosion resistance and mechanical properties[1-3]. SCC is the electrochemical anodic reaction under the action of corrosion environments, stress and material at the crack tip in nuclear pressure vessels and piping in high temperature water environment, which has become an important research field of the structural safety and service life of nuclear power plants[4-5]. However, how to improve the prediction accuracy of SCC growth rate is still a serious problem because of the numerous effect factors on SCC behaviours[6-7]. Mechanical state at the crack tip is one of the most important affecting factors in SCC crack growth rate, which is the topic focused on in this study.

2.Theory base of oxide film form and rupture

The theory of oxide film form and rupture has been widely used in quantitative prediction of the SCC growth rate of stainless steel and nickel base alloy in high temperature water environment. The morphology at the tip of SCC propagating is shown in Fig.1.Firstly, The oxide film at the crack tip is broken under the action of stress and strain. And then the broken part produces an anode reaction and the anode metal becomes ions and dissolves, and the crack tip is corroded to form a groove-type crack. Finally the oxide film reforms at the new crack tip. The SCC crack advance because this process is the cycle action and until the material failure[6-8]. The micro-mechanical state at the crack tip before and after oxide film rupture is discussed and analyzed in this paper.

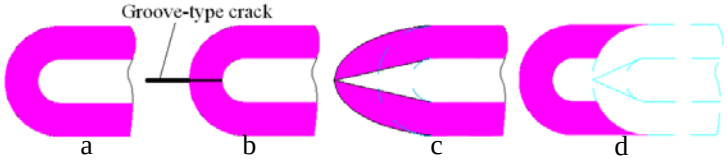

Fig.1 Sketch diagram of oxide film rupture and reform process
(a) Oxide film form;
(b) groove-type crack form;
(c) oxide film rupture
(d) oxide film reform

3.FEM model

3.1 Material model.

Ramberg-Osgood relation is used as the material mechanical relation of the Nickel base alloy and oxide film at SCC tip. The material mechanical parameters of nickel based metal 600, E is Young's modulus of the material and E=190GB; σo is the yield strength of the material and σo=436MPa; α is the yield offset and n is the hardening exponent for the plastic [9]. And the oxide film is regarded as a lineal-elastic brittle material, and its material mechanical parameters are, E=19GB, υ=0.3[6].

3.2 Geometry model and mesh.

One inch compact tension (1T-CT) specimen is used in this numerical calculation with the numerical experiment process according to the American Society for Testing and Materials Standard [10]. The geometric shape and size of 1T-CT specimen are shown in Fig.2(a).

The thickness of the oxide film at the SCC tip is assumed to be 2μm in this simulation. The groove-type crack length is arbitrary changed to 1, 2 and 3μm. Three stress observation paths are adopted in the oxide film, which is shown in Fig.2(b).

67020 CEP8 (8-node biquadratic plane stain quadrilateral) elements are adopted in the global model. Because the stress concentration appears in the boundary between the base metal and the oxide film at the SCC tip, the refined mesh is used nearby the crack tip, which is shown in Fig.2(c). The constant is loaded on specimen to keep the stress intensity factor is 30MPa·m1/2 [9].

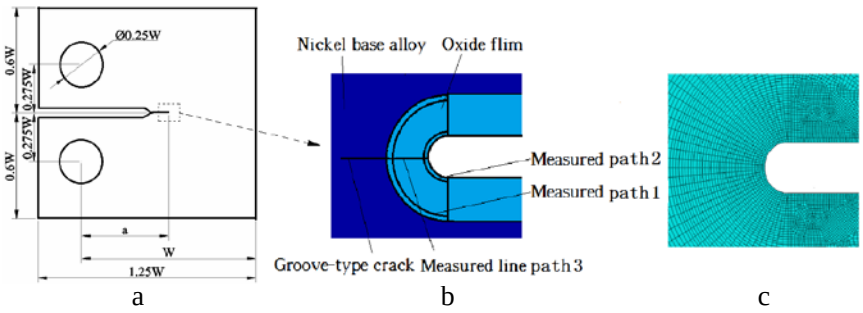

Fig.2 FEM model
(a) Geometric size of 1T-CT specimen (W=50mm, a=0.5W, c=1.5mm);
(b) groove-type crack model at SCC tip;
(c) FEM mesh nearby crack tip

4.Results and Discussions

4.1 Stress at the crack tip before the oxide film rupture.

In order to observe the morphology at the crack tip, the deformation is amplified 10 times. Stress nearby the crack tip before the oxide film rupture is shown in Fig.3. Stress in base metal is bigger than that in oxide film, and the maximum stress is nearby the oxide film boundary, and the maximum stress in oxide film is on the surface of film.

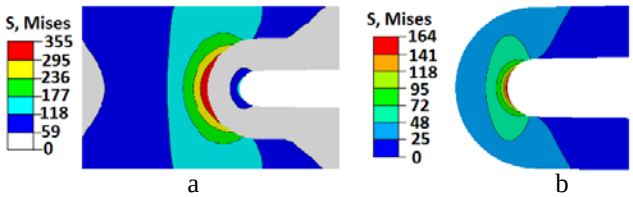

Fig.3 Stress nearby crack tip before oxide film rupture (MPa)
(a) Stress around crack tip;
(b) Stress around oxide film

4.2 Stress nearby the crack tip after the oxide film rupture.

In Fig.4, there are 5 contour lines represent the stresses are 0.2σ, 0.4σ, 0.6σ, 0.8σ and σ, respectively. The stress concentration transfers from the oxide film boundary to new crack tip when the groove-type crack occurs after the oxide film rupture. As the groove-type crack length advances, the maximal stress is removed from the oxide film boundary.

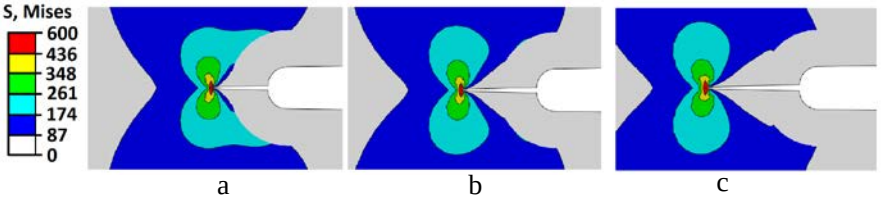

Fig.4 Stress nearby crack tip after oxide film rupture (MPa)
(a) groove-type crack is 1μm;
(b) groove-type crack is 2μm;
(c) groove-type crack is 3μm

As shown as Fig.5, the stress nearby the oxide film decreases as the groove-type crack length advances.

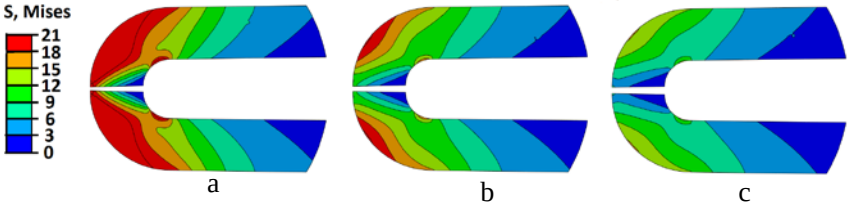

Fig.5 Stress nearby oxide film after oxide film rupture (MPa)
(a) groove-type crack is 1μm;
(b) groove-type crack is 2μm;
(c) groove-type crack is 3μm

4.3 Stress contrast nearby crack tip before and after oxide film rupture.

The stress of path 1 is shown in Fig.6. Before the oxide film rupture, the minimal stress appears in the direction of the crack growth. The stress distribution after the oxide film rupture is similar with that before the oxide film rupture. The shorter the groove-type length is, the bigger the stress is after the oxide film rupture.

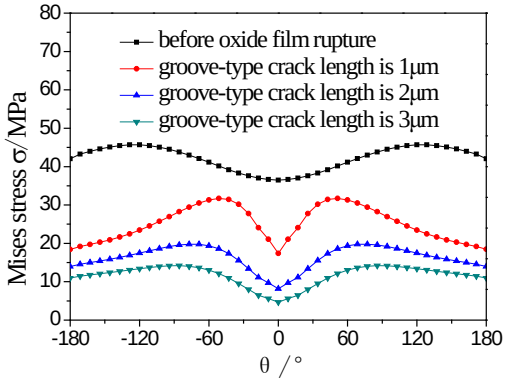

Fig. 6 Stress in path 1

The stress of path 2 is shown in Fig.7. Before the oxide film rupture, the maximal stress appears in the direction of the crack growth. The minimal stress is also the direction of the crack growth after the oxide film rupture, which is justly adverse with that before the oxide film rupture. The shorter the groove-type length is, the bigger the stress is after the oxide film rupture.

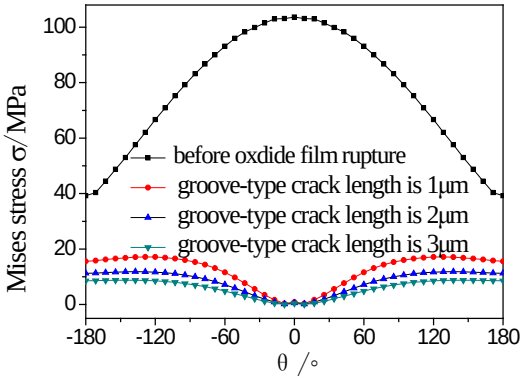

Fig. 7 Stress in path 2

The stress of path 3 is shown in Fig.8. The stress decreases as the distance from oxide film increases before the oxide film rupture, and the stress increases as the distance from oxide film increases after the oxide film rupture, which is adverse with that before the oxide film rupture . The shorter the groove-type length is, the bigger the stress is. In all of 3 paths the stress on oxide film before rupture is greater than that after rupture.

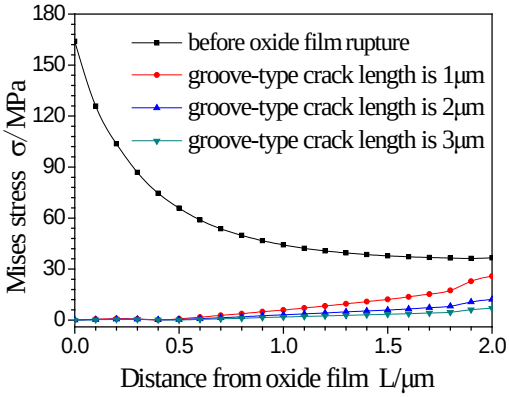

Fig. 8 Stress in path 3

Conclusions

By a comparative analysis of the stress at the SCC tip before and after oxide film rupture by using ABAQUS software, the following conclusions could be are obtained.

Before oxide film rupture, the maximal stress at SCC tip situate the base metal region nearby boundary between the oxide film and base metal, and after oxide film rupture, the maximal stress move forward as the groove-type crack advances.

It is similar that the stress trend along the boundary between the base metal and oxide film before and after oxide film rupture, but it is adverse that the stress trend along the free surface of the oxide film before and after oxide film rupture.

Acknowledgements

This work is financially supported by Natural Science Foundation of China under Grant No. 51475362 and Research Fund for the Doctoral Program of Higher Education of China under Grant No. 20136121110001.

References

[1] Xue,H. & Shoji T. Quantitative Predition of EAC Crack Growth Rate of Sensitized Type 304 Stainless Steel in Boiling Water Reactor environments Based on EPFEM, *Journal of Pressure Vessel and Technology Transactions of the ASME*, 129 (3), PP.460-467,2007.

[2] Lu,J.S., Wang,B.F. & Zhang,J.Y. A Review of Stress Corrosion Cracking Studies of Stainless Steels and Nikel Base Alloys in High Temperature Water. *Nuclear Power Engineering*, 22(3), pp.259-263,2001.

[3] Yan,F.Q., Xue,H., Zhao,L.Y. & Fang,X.R. Effects of Stress Intensity Factor on Electrochemical Corrosion Potential at Crack Tip of Nickel-Based Alloys in High Temperature Water Environments, *Rare Metal Materials and Engineering*, 44(3), pp.0513-0518,2014.

[4] Tu,S.D., Xuan,F.Z., & Wang,G.W. Recent progress in high tempterature mechanical behavior of materials and structures, *China journal of Solid Mechanics*, 31(6), pp.679-695,2010.

[5] Sato,Y., He, X., Takeda,Y. & Shoji, T. Development of a Stress Corrosion Crack Test Methodology Using Tube-shaped Specimen，*ASTM Journal of Testing and Evaluation*, 35, pp.254-258,2007.

[6] Andresen,P.L. & Ford,F.P. Modeling and Life Predicition of Stress Corrosion Cracking Predictive Capabilities in Enviromentally Assisted Cracking, *Proceeding of the ASME Pressure Vessels and Piping*, 99, pp.17-38,1985.

[7] Xue,H., Xue, X.F., Tang,W., Zhao,L.Y. & Gong,X.Y. Analysis on Mechanical Property of Oxide Film in Stress Corrosion Cracking Tip of Nicked-based Alloys, *Rare Metal Materials and Engineering*, 40(7), pp.1189-1190.

[8] Gong,M., Yu,Z.x. & Lin,C.*Theory of Metal Corrosion and Control*，Chemical Industry Press, Beijing, 2009.

[9] Tang,W., Xue,H., Zhao,D.,Shi,L.B. & Fang,X.R. Numerical analysis of the mesoscale mechanical field at the intergranular crack tip, *Proceeding of the ASME Pressure Vessels and Piping*, 3, pp.515-520.

[10] ASTM Standard E399-90. *Annual Book of ASTM Standards*, USA: ASTM International, 2002.

[11] Hibbitt, Karlsson & Sorensen, Inc. *ABAQUS/Standard User's Manual Version 6.5*. Pawtucket: ABAQUS, 2004.